The Functional Connectivity between the Locust Leg Pattern Generating Networks and the Subesophageal Ganglion Higher Motor Center

Daniel Knebel[†1,2], Jan Rillich[†1,3], Leonard Nadler[4]. Hans-Joachim Pflueger[4] and Amir Ayali[1,2]*

[1]Department of Zoology, Tel Aviv University, Tel Aviv, Israel.
[2]Sagol School of Neuroscience, Tel Aviv University, Tel Aviv, Israel.
[3] Institute for Biology, University of Leipzig, Leipzig, Germany.
[4]Institut für Neurobiologie, Freie Unversität Berlin, Berlin, Germany.

[†] These should be considered joint first author

* Author for Correspondence:
Amir Ayali
ayali@post.tau.ac.il

Acknowledgements

This work was partially supported by DAAD travel scholarships (to DK) and, in its final stages, by the German Research Council (DFG; Grant RI 2728/2-1). H-J P gratefully acknowledges the support by the DFG (FOR 1363, Pf128/30-1 and PF128/32-1) and the receipt of a Berlin NaFoeG-stipend to LN. We thank Baruch Barzel for his valuable support in the data analysis.

The authors declare no conflict of interests

Abstract

Interactions among different neuronal circuits are essential for adaptable coordinated behavior. Specifically, higher motor centers and central pattern generators (CPGs) induce rhythmic leg movements that act in concert in the control of locomotion. Here we explored the relations between the subesophageal ganglion (SEG) and thoracic leg CPGs in the desert locust. Backfill staining revealed about 300 SEG descending interneurons (DINs) and some overlap with the arborization of DINs and leg motor neurons. In accordance, in *in-vitro* preparations, electrical stimulation applied to the SEG excited these neurons, and in some cases also induced CPGs activity. Additionally, we found that the SEG regulates the coupling pattern among the CPGs: when the CPGs were activated pharmacologically, inputs from the SEG were able to synchronize contralateral CPGs. This motor output was correlated to the firing of SEG descending and local interneurons. Altogether, these findings point to a role of the SEG in both activating leg CPGs and in coordinating their oscillations, and suggest parallels between the SEG and the brainstem of vertebrates.

Keywords: locomotion, locust, insect, subesophageal ganglion, central pattern generator (CPG), intersegmental coordination

Introduction

A longstanding and fundamental question in neuroscience is that of how the brain coordinates motor behaviors (Penfield and Boldrey, 1937; Schmidt and Lee, 2005; Fritsch and Hitzig, 2009). Ample research across species and methodologies has revealed a differentiation between three levels of motor control: central pattern generators (CPGs - neuronal oscillators that can produce rhythmic motor output in the absence of sensory or descending inputs; see recent reviews in Marder and Bucher, 2007; Mulloney and Smarandache, 2010; Marder, 2012; Rybak et al., 2015); sensory feedback; and higher motor centers. In most cases, the CPGs determine rhythmic alternating activity of specific antagonistic muscles. The CPGs by themselves, or often together with a few of the many sensory feedback loops in intact animals, are sufficient for the generation of coordinated motor patterns (e.g. Bal et al., 1988; Stevenson and Kutsch, 1987). Higher motor centers, on the other hand, have a wide-ranging influence, affecting various body parts concurrently. They may select the appropriate behavior, initiate it, and orchestrate it. To this end, higher motor centers form functional connections with CPGs and may modulate different ones simultaneously. This report describes the interplay between leg CPGs and subesophageal ganglion (SEG), which serves as a higher motor center for locomotion (Gal and Libersat, 2006; Kaiser and Libersat, 2015; Tastekin et al., 2015), of the desert locust, *Schistocerca gregaria* (Forskål).

A comprehensive body of work describing the interactions between higher motor centers and CPGs in the tadpole largely inspired our current work, which shares similar aims with it. Each of the tadpole's spinal cord segments includes two CPGs that produce an alternating rhythmic motor output, activating the myotomal muscles and thus inducing stereotypic swimming movements (Kahn and Roberts, 1982a). These segmental circuits reciprocally inhibit each other, while maintaining a phase difference between the activity of consecutive segments, thus producing the longitudinal directionality of the movement (Kahn and Roberts, 1982a; b). However, when the spinal cord is isolated from the hindbrain, only short fictive swim bouts can be generated (Li et al., 2006). Further research into these findings revealed that in addition to the spinal network of CPGs, another rhythm-generating center resides in the hindbrain, consisting of electrically coupled descending interneurons (DINs), which are active before each cycle of the spinal

motor output, and drive the spinal CPGs (Li et al., 2006, 2009, 2010; Soffe et al., 2009). Similarly, studies in mice and lampreys have pointed to an instrumental role of the brain stem in locomotion (McClellan and Grillner, 1984; Dubuc et al., 2008; Gordon and Whelan, 2008; Hägglund et al., 2010).

To date, the study of higher locomotion centers in insects has mostly focused on their behavioral role *in-vivo*. Using lesions, genetic techniques, and electrophysiological recordings, certain areas of the insect supraesophageal ganglion (brain), such as the central complex and mushroom bodies, were shown to control advanced aspects of walking: for example, speed change and turning (e.g. Strauss, 2002; Gal and Libersat, 2006; Poeck et al., 2008; Bender et al., 2010; Guo and Ritzmann, 2013). The SEG, which anatomically resides between the brain and the thoracic ganglia, was considered responsible for more basic features of walking such as initiation, maintenance, and forward-backward orientation (Huber, 1960; Kien and Altman, 1984; Bässler et al., 1985; Kien, 1990a; Gal and Libersat, 2008; Bidaye et al., 2014). In accordance, lesion-based experiments have demonstrated that removal of the brain does not abolish spontaneous walking, whereas the removal of the SEG eliminates it (Kien and Williams, 1983; Gal and Libersat, 2006). Our knowledge of the anatomical and moreover functional connections between the SEG and leg CPGs is, however, still incomplete.

In accord with previous studies that found central connections between the locust limbs (e.g. Berkowitz and Laurent, 1996), we have recently offered a detailed description of the functional connections among the inter-leg coxa-trochanteral CPGs in the locust *in-vitro* (Knebel et al., 2017). We showed that each of the three thoracic ganglia has its own default, inherent, bilateral coupling of these CPGs: in-phase within the pro- and mesothoracic ganglia, and anti-phase in the metathoracic ganglion. Furthermore, each ganglion was found to be capable of imparting its coupling scheme onto the other ganglia. Importantly, as in most walking systems (Büschges et al., 2011), none of the observed *in-vitro* inter-leg coordination schemes resembled a functional walking gait, and specifically not the tripod gait common among insects, in which neighboring pairs of legs show antiphase activity (Wilson, 1966; Grabowska et al., 2012). The thoracic network of oscillators must, therefore, feature inherent flexibility in order to establish a functional walking gait.

In the current report we follow-up on this work, taking advantage of the locust's easily accessible nervous systems, as well as its anatomical modularity, i.e. the functional and anatomical separation of the leg CPGs, compartmented by the three interconnected segmental thoracic ganglia; and the higher locomotion centers, encompassed in the two head ganglia – the brain and SEG (or gnathal ganglia; Ito et al., 2014). We introduce first evidence of leverage points for central regulation of the leg CPG network by the SEG higher motor center.

Materials and Methods

Experimental animals

All experiments were performed on adult male desert locusts (*Schistocerca gregaria*) from our colony at Tel Aviv University (Ayali and Zilberstein, 2002), within the first two weeks after the final molt. All experiments complied with the Principles of Laboratory Animal Care and the Israeli Law regarding the protection of animals.

Preparation

Recordings were conducted from *in-vitro* ventral nerve chord preparations, including the pro-, meso- and metathoracic ganglia, and the SEG. Prior to dissection, the animals were anesthetized with CO_2 for at least 5 min. Following removal of the brain (decerebration), appendages, the pronotal shield, and the abdomen posteriorly to the fourth abdominal segment, a longitudinal cut was performed in the cuticle along the dorsal midline of the thorax. The preparation was pinned to a Sylgard dish (Sylgard 182 silicon Elastomer, Dow Corning Corp.), and the cut was widened and superfused with locust saline containing (in mM): 150 NaCl, 5 KCl, 5 $CaCl_2$, 2 $MgCI_2$, 10 Hepes, 25 sucrose at pH 7.4. Air sacs and fatty tissue covering the ventral nerve cord were removed, and the thoracic ganglia chain and SEG with their surrounding tracheal supply were dissected out of the animal body, pinned in a clean Sylgard dish, dorsal side up, and bathed in locust saline. The two main tracheae were opened and floated on the saline surface. All peripheral nerve branches originating from the thoracic ganglia were cut short except for the N5a nerves (numbered after Campbell, 1961), which each contain

three motor axons: the slow and fast trochanteral depressors and a common inhibitor (Fig. 1; Ds, Df, and CI respectively).

Electrophysiology and neuroanatomy

To test the effect of SEG electrical stimulation on the thoracic motor output, trains of short electrical pulses (200 ms of 250 Hz pulses of 0.5 ms each, 1 V) were delivered to different areas of the SEG by carefully-fashioned insulated platinum-iridium electrodes, with especially high resistance and small tip diameter (15 μm), as described by Hussaini and Menzel (2013). Thus, we limited the stimulated area as much as possible. All electrical stimulations were generated by a Master 8 stimulator (A.M.P.I).

The activity of the motor nerves (N5a) of each thoracic ganglion was extracellularly recorded by suction electrodes made of borosilicate glass capillaries (A-M systems) and pulled with a P87 puller (Sutter Instruments). Unipolar hook electrodes were used to monitor inter-segmental information transfer from the inter-ganglia connectives (SEG-pro, pro-meso, meso-meta). Data were acquired using two four-channel differential AC amplifiers (Model 1700, A-M Systems).

For intracellular recordings, the SEG neurons were impaled with borosilicate glass capillaries pulled with the P87 puller. The electrode tips were filled with 3 % Neurobiotin (Vector Laboratories, Inc.) diluted in 3M potassium acetate and the shafts with 3M potassium acetate alone, leaving a small air bubble in between. These electrodes had a resistance of approximately 60 MΩ. In order to penetrate the ganglion sheath, a few crystals of protease (Sigma-Aldrich) were placed on the ganglion for 30 s. Intracellularly recorded signals were amplified using a DC amplifier (Axoclamp-2B, Molecular Devices). All recordings were digitized (Axon Digidata 1440A A-D board) and stored on a computer using standard software (Axo-Scope software; Molecular Devices). Resting membrane potentials for all intracellular recordings shown were below -65 mV. After evaluating the responses to restricted drug application, the intracellularly recorded neuron was labeled by iontophoretic injection of Neurobiotin using depolarizing current pulses (2 nA; 100 ms; 5 Hz; 20-40 min).

Backfill staining was accomplished by cutting the desired nerve and bathing it in Dextran-Rhodamine (Molecular probes) or Neurobiotin. After intracellular labeling or

backfill staining, preparations were placed for 24 h in a moisture chamber at 4°C to allow the tracer to diffuse along the neurons. Thereafter, the nerve chord was fixed for 2-4 h in 3% paraformaldehyde. The ganglia sheaths were permeabilized with a 0.1% collagenase/dispase (Sigma-Aldrich) solution for 30 min at 36°C before the Neurobiotin labeling was visualized by streptavidin-Cy3 (Jackson ImmunoResearch Labs). Finally, the ganglia chain was dehydrated in an ethanol series and cleared in methyl-salicylate (Merck KGaA). The whole-mount preparations were scanned with a confocal microscope (either ZEISS LSM 510, Carl Zeiss, or LEICA TCS SP2, Leica). Neurons were reconstructed from confocal image stacks using Fiji software (http://fiji.sc/wiki/index.php/Fiji).

Pharmacological treatment

The muscarinic receptor agonist pilocarpine hydrochloride (Sigma-Aldrich, St Louis, MO, USA) was dissolved in locust saline to a final concentration of 0.5 mM, which typically elicits rhythmic motor activity in leg motor nerves (e.g. Ryckebusch and Laurent, 1993). After 5 min in normal saline, the pilocarpine solution was restrictively bath-applied to the metathoracic ganglion, which was isolated from the rest of the ventral nerve cord by surrounding it with a petroleum jelly (Vaseline) wall. All other thoracic ganglia and the SEG were bathed in normal saline. The well was carefully leak proofed by applying saline, first only to the surrounding of the well, then into the well only, and checking for leaks from the well walls.

Data analysis

The pilocarpine-induced motor activity in the thoracic ganglia was measured in 31 experiments, initially with the SEG intact and subsequently again after disconnecting the SEG. In each experiment between three to seven simultaneous recordings were conducted from the leg depressor motor neuron (MN) pools, including the slow and fast trochanteral depressors and common inhibitor (Fig. 1; Ds, Df, and CI respectively). Spikes were detected and identified based on their amplitude, and only activity of the excitatory MNs was taken into account, without separating between the Ds and Df. Additionally, in some of the experiments the activity of the inter-ganglia connectives and SEG interneurons was

199 also monitored. We routinely evaluated the activity in two subsequent 8 min windows:
200 the first, typically after 22 min post drug application, and the second immediately after
201 the neck connectives were cut.

202 To identify SEG DINs in the connective recordings, spikes were first identified
203 using a template recognition function (Dataview software, University of St. Andrews) in
204 one of the channels. Subsequently, we overlaid all identified spikes in 20 ms windows by
205 aligning their maximum point. We repeated this process for the parallel time windows in
206 the other connectives recordings, and averaged each of the overlays. This allowed us to
207 examine the typical activity before and after the identified spike in the more rostral and/or
208 caudal connective recordings. Based on a typical axonal conduction speed of 2 m/s
209 (Gray and Robertson, 1998), and a distance of 3-5 mm between each pair of electrodes,
210 we expected DINs spikes to appear at a delay of about 1.5-2.5 ms between electrodes
211 monitoring adjacent ipsilateral connectives, from rostral to caudal. Spikes that were not
212 accompanied by such preceding or delayed activity in adjacent connectives were filtered
213 out. In one experiment, we used hook electrodes to record both neck connectives and to
214 identify simultaneous bilateral descending spikes. After verifying that the spike was
215 descending (as described above), we selected only simultaneous spikes in both
216 connectives.

217 To characterize the phases between the output of pairs of CPGs, we used cross-
218 spectrum analysis in MATLAB (MathWorks Inc.), following a procedure developed by
219 Miller and Sigvardt, (1998; see also Sigvardt and Miller, 1998). Only significantly
220 coherent frequencies of each pair of recordings were used to calculate each experiment
221 mean phase vector. The Watson–Williams F-test was used to test for differences in the
222 phase vectors. In order to combine both the uniformity and directionality of the phase
223 distributions, we used the synchronization index, ranging from -1, perfect anti phase, to
224 +1, perfect in phase. This was calculated by averaging all the experiments mean phase
225 vectors, and projecting the product on the 0-180 axis (see Knebel et al., 2017 for more
226 details on the cross-spectrum and synchronization index).

227 In order to compare the SEG neuronal output and the activity of thoracic MN pools,
228 we utilized cross-covariance analysis in MATLAB. We used a smoothed on-time vector
229 of the spikes of each of the simultaneous recordings. It should be noted that the resultant

covariance coefficient value was normalized in order to be able to compare between different analyses. The coefficient is valid only relatively as it is highly dependent on the prior smoothing process: the change of the coefficient over time represents the relative likelihood of spikes to occur in different temporal circumstances, and can be compared among the different examples presented that went through the exact same process.

We tested the statistical significance of the obtained covariance coefficients by performing the exact same analysis on 1000 randomly chosen pairs of the motor output recordings, in which each recording came from a different experiment (different locust). Thereby, we could calculate a bootstrap which represented a confidence interval of 95%, which defined the range of covariance coefficients that could be obtained by chance (<95%). The extreme values of the bootstrap were 1.11 and -0.968. Thus, any result that crosses these have less than a 5% chance of being a type 1 error, and therefore can be considered statistically significant. All the results which are mentioned as meaningful crossed this threshold, unless noted otherwise.

To merge the cross-covariance of the activity of two MN pools and SEG neuronal activity, we multiplied the two normalized cross-covariances calculated separately for each MN pool against the SEG neuronal activity. This yielded a square matrix, in which the axes represent the lags of each cross-covariance. Thus, the diagonal axis (from bottom left to top right) depicts the on-time correlation of the MN pool in respect to the SEG activity, while any deviation from this line indicates the correlation value at a certain time-lag. Again, the absolute values of this analysis are relative, but can be compared among themselves to show the tendency of firing at different temporal states of the network.

Results

All electrophysiological experiments (N=40) were performed on isolated ventral nerve cords of the locust, including the SEG and the three thoracic ganglia. In all, we evaluated the activity of the coxa-trochanteral CPGs, which induce alternated motor output between the leg levator and depressor motor neuron pools (Ryckebusch and Laurent, 1993; Rillich et al., 2013; Knebel et al., 2017). Based on this robust motor pattern, we measured the activity of trochanteral depressor MNs as representatives of the

leg motor output, which participate, among others, in the stance phase during stepping.

The DINs deliver the SEG descending control of the thoracic motor centers

The SEG higher motor center commands are delivered downstream to the peripheral motor center via a set of DINs (Kien, 1990a; b; Kien et al., 1990; Gal and Libersat, 2006). We performed three experiments in which we stained one neck connective, and found 146, 153, and again 153 stained neuronal somas in the SEG (example: Fig. 1A). Therefore, assuming symmetry, and taking into account the few neurons that send descending neurites in both connectives, there are almost 300 SEG DINs (in accordance with Kien et al., 1990). To explore the anatomical relations between the head ganglia DINs and the leg depressor MNs, we performed a double labeling of the metathoracic N5a nerves and one neck connective. This revealed that many DIN projections overlap with the arborization area of the N5a neurons, both ipsilaterally to the stained connective and contralaterally (Fig, 1B and C). We could not determine whether the DINs originate in the brain or the SEG, or whether they form synapses with the motor neurons. However, the overlapping between DINs' projections and the leg motor neurons are consistent with the previously reported functional connections, both for the SEG DINs (cockroach: Gal and Libersat, 2008; locust: Kien, 1983; Kien and Altman, 1984) and the brain DINs (cockroach: Bender et al., 2010; Mu and Ritzmann, 2008; Ridgel and Ritzmann, 2005).

The intact SEG fails to induce activity in the thoracic ganglia chain

Previous studies have shown that headless insects, lacking both the supra- and subesophageal ganglion, do not engage in spontaneous walking, and upon tactile stimulation walk only briefly. However, when the SEG was left intact, the insects tended to walk spontaneously and often uninhibitedly, without any additional stimulation (e.g. stick insect: Bässler, 1983; locust: Kien, 1983; cockroach: Gal and Libersat, 2006). Accordingly, several studies have also reported that without the SEG the leg CPGs are inherently inactive *in-vitro* (Knebel et al., 2017 and references within). Therefore, we

first explored whether the intact SEG induces spontaneous fictive leg motor activity in the *in- vitro* thoracic ganglia chain preparations.

In all experiments (N=40) the pro- and mesothoracic ganglia depressor MN pools were silent, whereas the meta-thoracic slow depressor was tonically firing (examples: Fig. 1D and E before the stimulus; see also Knebel et al., 2017; Rillich et al., 2013). No spontaneous motor bursts of action potentials were evident in any of the recordings.

Stimulation of the SEG labial neuromere is sufficient for generating leg CPGs activity *in-vitro*

Extracellular electrical stimulation of the SEG was previously reported to evoke bouts of walking in semi-intact locusts (Kien, 1990a). Following this report, we sought to explore the effect of electrical stimulation to the SEG *in-vitro*. A pair of fine electrode was positioned into the SEG by way of a micromanipulator, and trains of short electrical pulses were applied, while the thoracic motor output was recorded. Due to the easy accessibility of the isolated preparation, we were able to direct the stimulating electrode to any of the three SEG neuropiles (the mandibular, maxillar, and labial neuromeres, from rostral to caudal). Furthermore, we were able to position the electrode in an area very close to the SEG longitudinal midline, and together with the high resistance small tip electrode used, the possible stimulation of the lateral tracts, in which most axons of brain DINs run directly to the ventral nerve cord, was limited.

Short electrical stimulations were delivered to 2-3 of the SEG neuromeres in four animals. Each trial consisted of 10 stimulations at intervals of 30 sec. In all experiments, a motor response in at least one thoracic ganglion was recorded. However, stimulation of the different neuromeres evoked different motor outputs: The mandibular and maxillar stimulations resulted in short responses (example of a mandibular stimulation: Fig. 1D; overall medians: mandibular 1.4 sec and maxillar 4.1 sec), whereas the labial stimulation elicited prolonged activity with an overall median of 22.9 sec. Moreover, stimulation of the labial neuromere elicited rhythmic bursting activity of up to six bursts, in 2-4 of the recorded thoracic leg CPGs (example: Fig. 1E).

Rhythmic bursting activity in a sensory-deprived preparation is necessarily the product of CPG activation. Our findings thus indicate that the labial neuromere of the

318 SEG is sufficient to activate the leg CPGs in all three thoracic ganglia. Interestingly,
319 during all the *in-vitro* labial neuromere stimulations we observed prothoracic bilateral
320 synchronized excitation, whereas coupling patterns among the other recorded nerves
321 were varied (example: Fig. 1E).

322 **The SEG has no effect on specific bursting properties of the leg CPGs**

323 The muscarinic agonist pilocarpine is known to activate leg CPGs in isolated
324 nervous systems of arthropods (Chrachri and Clarac, 1987; Ryckebusch and Laurent,
325 1993, 1994; Ryckebusch et al., 1994; Büschges et al., 1995; Johnston and Levine, 2002;
326 Fuchs et al., 2011, 2012; Rillich et al., 2013; David et al., 2016). Recently, we
327 demonstrated that applying pilocarpine restrictively to each of the thoracic ganglia is
328 sufficient for inducing activity in all leg CPGs, including those of the untreated ganglia
329 (Knebel et al., 2017). To explore a tentative effect of the SEG on the CPG-CPG
330 interactions, we activated the thoracic CPGs by applying pilocarpine to the metathoracic
331 ganglion alone in an *in-vitro* preparation, and compared the motor output of the different
332 depressor MN pools both with the SEG intact and following its removal. Thus, while the
333 generation of rhythmicity arose from the caudal end of the ganglia chain, any SEG
334 modulatory influence had to be sent from the rostral end (pictogram: Fig. 2A).
335 Following pilocarpine application, rhythmic motor patterns were obtained in all
336 thoracic ganglia within 2-5 min (Fig. 2A). Before analyzing the coordination pattern
337 among the bursts of the different hemiganglia, we examined whether the SEG influences
338 the general properties of each CPG activity. To this end, we compared the spike
339 frequency in each recording, before and after SEG removal, and found no significant
340 change (Fig. 2B; N=31). We further examined the influence of the SEG on the CPGs
341 recruitment to the pharmacologically activated metathorcic CPGs; as only the
342 metathoracic ganglion was directly exposed to pilocarpine, all other CPG activity resulted
343 from activation of its CPGs. Therefore, the frequencies of the metathoracic CPGs and the
344 other CPGs should resemble each other (i.e. share a common frequency). Using the cross-
345 spectrum analysis, we tested whether the common frequencies differed with and without
346 the SEG (Fig. 2C). We found no effect of the SEG removal on the most common
347 frequencies in the meta-prothoracic and meta-mesothoracic bursting activity (N=31), and

348 therefore concluded that the SEG does not affect the frequency-entrainment of the rostral
349 CPGs by the caudal metathoracic source of rhythmicity. Additionally, we found no SEG
350 effect on the shared frequencies between the two contralateral metathoracic CPGs.
351 Therefore, the SEG has no influence on the rhythmicity of the CPG network.

352 **The SEG modulates phase parameters among the CPGs**

353 As noted, we have recently reported that in *in-vitro* preparation, when pilocarpine
354 was applied onto the metathoracic ganglion only, all the ganglia bilateral CPGs oscillate
355 in antiphase while the ipsilateral CPGs are synchronized (Knebel et al., 2017). Here we
356 further explored whether the SEG is able to affect this coordination pattern. To this end,
357 we used the synchronization index to determine the synchrony level between each couple
358 of oscillators in our experiments (see Methods for details).
359 In line with our previous results, when the metathoracic ganglion was directly
360 activated with pilocarpine and the SEG was intact, all ipsilateral CPGs fired bursts of
361 action potentials in-phase. However, unlike in our previous report, in the presence of the
362 SEG the bilateral CPG also oscillated and fired in-phase (Fig. 3C). After removing the
363 SEG, while the ipsilateral CPGs oscillations remained synchronized, the activity of the
364 contralateral CPGs shifted towards anti-phase (Fig. 3D), similar to that recorded in our
365 previous report (where the SEG was removed at the dissection stage; Fig. 3E). Most
366 prominent was the change in the prothoracic ganglion CPGs, whose synchronization
367 index significantly dropped from 0.61 to -0.24 following SEG removal.
368 Taken together, the SEG synchronizes the activity of the two lateral sides of the
369 CPG network, without affecting the capacity for frequency entrainment and the burst
370 properties of the CPG network.

371 **Candidate SEG interneurons participate in the bilateral synchronization**

372 To explore the underlying neuronal circuitry behind the bilateral synchronizing
373 effect of the SEG, we simultaneously recorded the CPG motor outputs and the inter-
374 ganglia connectives. Based on multiple connective recordings (example: Fig. 2A) and
375 subsequent spike sorting, we were able to extract the activities of single SEG DINs.
376 Figure 4A-D presents an example of such SEG DIN activity. The cross-covariance

377 analysis shows that this DIN activity was correlated with the firing of the two bilateral
378 MN pools in the prothoracic ganglion: that ipsilateral to the connectives recorded, and
379 that contralateral to them (Fig. 4B). The correlation of the DIN with the latter showed a
380 slight but consistent delay. This difference is visualized in the merged cross-covariance
381 shown in Fig. 4D, where the blue spot, representing a higher correlation between the ipsi-
382 and contralateral prothoracic MN pools in relation to the DIN firings, is smeared towards
383 the positive values of the contralateral prothoracic axis. Since the cross-covariance
384 between the DIN and the metathoracic CPG did not reveal a temporal relationship
385 between their activities (Fig. 4B, green line), this DIN activity is correlated to the activity
386 of specific CPGs.

387 By means of intracellular recordings we obtained further insights into the activity
388 of SEG interneurons during the metathoracic pilocarpine-induced rhythm. Figure 4E
389 presents an example of a SEG DIN recording. This cell's activity resembled that of the
390 DIN described above, as can be seen in the cross-covariance analysis: correlated activity
391 with both pro-thoracic MN pools, with a slight difference in the shape of the correlation
392 over time, and only weaker correlation with the metathoracic MNs (Fig. 4F). The
393 recording exhibits rather small action potentials and robust changes in the membrane
394 potential, indicating soma rather than axonal recordings. Hence, to correlate this DIN
395 activity with the prothoracic motor output, we used the values of the membrane potential
396 (and not only the spike on-times).

397 The two examples presented above demonstrate correlations between the output of
398 both of the prothoracic hemiganglia and an SEG DIN. However, in both cases, the left
399 and right CPGs were rather synchronized even irrespective of the DIN activity (Fig. 4C
400 and G), and it is impossible to distinguish whether the DINs' activity was connected to
401 one or both the prothoracic CPGs. Therefore, we further analyzed the findings from other
402 experiments, in which the CPG-GPG correlation was lower. Figure 4I presents an
403 example of an intracellular recording of an SEG interneuron in a preparation, in which
404 the prothoracic bilateral synchronization was relatively small (Fig. 4K). Nonetheless,
405 each of the prothoracic CPGs showed correlation with the SEG interneuron (Fig. 4J).
406 Moreover, the merged cross-covariance visualizes the small time window, in which the
407 SEG interneuron was correlated with both prothoracic CPGs (Fig. 4L), in contrast to the

overall low bilateral correlation. These findings suggest that this SEG neuron interacts with both prothoracic MN pools.

SEG descending dorsal unpaired median (DUM) neurons interact with the CPG network

The coupling between independent CPGs can be modulated by neuromodulators such as the biogenic amine octopamine (e.g. Rand et al., 2012; Rillich et al., 2013). To determine whether octopaminergic SEG neurons are centrally coupled to the leg CPGs and are possibly involved in their synchronization, we aimed at specifically recording the octopaminergic SEG DUM neurons.

Due to their unique bilateral descending neurites (Kien et al., 1990; Bräunig, 1991; Cholewa and Pflüger, 2009), we were able to identify the DUM neurons' activity by recording from both neck connectives, and from the pro-meso connective simultaneously (see Methods for details; Fig. 5A; the different spike amplitudes seen in the left and right connectives in this example is probably a result of different positions of the hook electrode on the two connectives;). Repeating the cross-covariance analysis for this DUM neuron and the two prothoracic CPGs indeed revealed a relatively strong correlation among the activity of all three (Fig. 5B and D). In this example, again, the correlation of each of the prothoracic CPGs with the DUM neuron exceeded the correlation between both CPGs (Fig. 5C).

Additionally, we intracellularly recorded from a SEG DUM neuron as confirmed by its labeling and action potentials (Fig. 6A): the neuron had a large soma of about 45 µm in diameter, was located medially on the dorsal posterior side of the SEG, and had a symmetrical arborization pattern in the SEG, similar to those described by Bräunig (1991; see laso Kien et al., 1990 and Bräunig and Burrows, 2004). Furthermore, its action potentials were long lasting (~3.5 ms; Fig. 6B), and its soma was excitable (Fig. 6F), as typical for DUM neurons (soma spikes: Heidel and Pflüger, 2006). Similar to the DUM neuron identified by recording the connectives spikes (Fig. 5), this neuron's action potentials showed a tendency to be synchronized with the output of both prothoracic CPGs (The correlation was statistically significant only with the left nerve recording), while the activity of the CPGs themselves was not correlated (Fig. 6C and D).

In order to uncover the postsynaptic potentials (PSPs) that this neuron receives, we hyperpolarized it for several minutes and thus minimized the action potentials generated. We found that the DUM neuron received accurate and consistent information about co-activation of the two prothoracic CPGs (example: Fig. 6G; analysis: Fig. 6H). Since the DUM neuron EPSPs indicate synchrony between the bilateral CPGs, they might offer a mean of coincidence detection. Interestingly, during the period of hyperpolarization, the synchronization among the prothoracic CPGs noticeably increased (Fig. 6I). Depolarization, on the other hand, did not evoke any immediate response (Fig. 6F).

Discussion

In this study we have demonstrated two major aspects of functional interactions between the higher locomotion centers of the SEG and the leg CPGs in the locust: (1) the ability of the SEG to induce CPG activity, and (2) the role of the SEG in coordinating the coupling among the leg CPGs. These interactions are mediated by the SEG DINs, connecting the SEG with the thorax.

The use of *in-vitro* preparations

All the experiments presented here were conducted *in-vitro*. As previously explained in Knebel et al. (2017), and as a common working hypothesis in CPG research (e.g. Ayali and Lange, 2010 for review), it is advantageous to study the central interplay of CPGs in the complete absence of sensory inputs. This reductionist approach is consistent with the very definition of CPGs as a neuronal oscillator capable of performing its tasks with no sensory regulation (Marder and Bucher, 2001). However, there are also some clear limitations to this approach: namely, that conclusions, valid at the level of the neuronal network and nervous system, may not be directly reflected in the actual behavior, which is further shaped by additional sources, such as sensory inputs and the animal's internal state, in the intact animal. Nonetheless, it is important to note that since the central connections and interactions we studied here *in-vitro* are those underlying the execution of the motor behavior, the insights gained *in-vitro* are instrumental for the

466 generation of hypotheses and predictions regarding *in-vivo* insect locomotion.

467 **The SEG's ability to initiate different activity patterns in leg CPGs**

468 By means of electrical stimulation of SEG neurons we were able to activate each of
469 the leg coxa-trochanteral CPGs. This finding, obtained in the isolated *in-vitro*
470 preparation, indicates the sufficiency of the central connections between the SEG and the
471 thoracic ganglia in activating the leg CPGs. Moreover, of the three SEG neuromeres,
472 overall containing approximately 300 SEG DINs (Fig. 1A; see also Kien et al., 1990), we
473 identified the labial neuromere as the most potent SEG area for CPG activation. Labial
474 neuromere excitation induced prolonged bursting rhythms, similar to those obtained by
475 activating the leg CPGs pharmacologically (compare examples in Fig. 1E and Fig. 2A;
476 see also Knebel et al., 2017). These results are in accord with those reported by Kien
477 (1983), as well as with our own preliminary experiments (not described herein), showing
478 that stimulating the SEG in a semi-intact preparation results in leg movements (suppl.
479 videos 1&2). Altogether, these findings suggest that the SEG is capable of inducing leg
480 CPGs activity, and thus initiating stepping behavior. Moreover, they also suggest that by
481 providing rhythmical excitatory and inhibitory signals to the leg CPGs, the SEG can
482 maintain ongoing legged activity, as was previously suggested by Kien and Altman
483 (1992). However, we also observed that intact connections to the unstimulated SEG were
484 not sufficient by themselves to initiate spontaneous leg motor activity. It therefore seems
485 that rather than constituting an autonomous "motivation center", the SEG functions as a
486 relay station or a mediator, and depends on central inputs from the brain, from other
487 CPGs, or on sensory information, in order to drive leg CPGs, (see also Kien and Altman,
488 1984). Moreover, the motor output induced by the SEG *in-vitro*, was monitored in all the
489 leg CPGs but did not resemble any functional walking gait. This indicates that there is no
490 complete "coordination program" or "walking motor program" conveyed by the SEG to
491 the CPG network. Nonetheless, throughout our experiments, a stereotypic bilateral
492 synchronization pattern of the leg CPGs was induced, suggesting that the SEG can
493 modulate the overall coordination of the locomotion network.
494 We have tried to limit the likelihood of stimulating severed axons, which originally
495 traveled from the brain to the SEG or thoracic ganglia, as explained in the methods and

results sections. However, as with any extracellular stimulation, we cannot rule out the possibility that undesired neurites were stimulated. Yet, our finding that the stimulation of different neuromeres resulted in differentiated activation of the legs MN pools, and that the coordination pattern established resembled that induced by the unstimulated SEG, indicates that at least to the degree of affecting the leg motor output, stimulation of brain DINs did not occur.

The SEG bilateral synchronizing influence

We characterized the role of the SEG in modulating the output of the leg CPGs network using an *in-vitro* preparation that included the thoracic ganglia and the SEG. Based on our previous study (Knebel et al., 2017), we chose a specific paradigm of restrictive pilocarpine application to the metathoracic ganglion. This allowed us to investigate the output of the more rostral pro- and mesothoracic ganglia, their interconnections, and their connection with the SEG, in the absence of any direct effects of pilocarpine.

We found that the SEG does not alter the firing properties of any individual CPG, nor their mutual bursting frequencies (Fig. 2B and C, respectively) but, rather, selectively affects the phase relations of the bilateral CPG couples, most consistently those of the prothoracic ganglion (Fig. 3). It is possible that the SEG can strengthen the inherent synchronized bilateral coupling of the prothoracic CPGs (Knebel et al., 2017), and the prothoracic ganglion, in turn, induces this coupling pattern upon its neighbors through the synchronizing ipsilateral connections. However, from the neuronal network perspective, since the ability of all the ganglia to induce activity in the CPGs of other ganglia and influence their phase is equal (Knebel et al., 2017), it is more plausible that the SEG modulates all bilateral inter-CPG connections, and that of the prothoracic ganglion is simply the most responsive. Moreover, the SEG had no noticeable effect on coupling among the ipsilateral CPGs, whose activities are synchronized independently of it. It should be noted that these findings were obtained without the animal's brain, and future studies will investigate its role in the CPGs coordination.

Supporting the findings described above, we found various examples of SEG cells (Fig. 4-6) whose activities increased in phase with the synchronized output of the left and

526 right prothoracic CPGs. In some of these examples, the correlations of the left and right
527 depressors with the SEG neurons were stronger than their mutual correlation (Fig. 4I-L,
528 5-6), suggesting that SEG neurons play an active role in bilateral synchronization.
529 However, due to the unexcitable properties of the soma membrane of those interneurons,
530 we were unable to elicit action potentials in most of our intracellular experiments, and
531 thus could not reach any causative conclusions regarding their role in the network.

532 It should be noted that due to our experimental procedure of restrictive
533 pilocarpine application, all correlated activity of SEG interneurons with the leg CPGs
534 must be the result of ascending information reaching the SEG and mirroring the CPG
535 activity. Such information can be referred to as “efference copy” (Jeannerod and Arbib,
536 2003), and is independent of sensory information (which was unavailable in our
537 experiments).

538 **The octopaminergic system interplay with the coordination of leg CPGs**

539 A potential candidate for the modulation of CPG-CPG interplay in insects is the
540 octopaminergic system (e.g. Rand et al., 2012; Rillich et al., 2013) and its prominent
541 members, the DUM neurons (for review: Libersat and Pflueger, 2004). Indeed, we found
542 that the activity of a descending SEG DUM neurons was correlated with the bilaterally
543 synchronized activity of the contralateral prothoracic CPGs (Fig. 5-6). This suggests
544 involvement of the octopaminergic system in the inter-CPG coordination, as all DUM
545 neurons in the SEG are octopaminergic (Bräunig, 1991; Stevenson and Sporhase-
546 Eichmann, 1995). Furthermore, we found that EPSPs recorded from a DUM neuron
547 reliably reflected the co-activation of the front leg depressors. Therefore, an ascending
548 neuron, or neurons, form synapses on the DUM neuron, eliciting changes in its
549 membrane potential correlated with the thoracic CPGs activity. This further confirms our
550 claim that a central efference copy of leg activity is delivered to the SEG.

551 Surprisingly, we found that upon silencing this DUM neuron, the prothoracic
552 bilateral synchronization increased. Taken together with the rest of our findings, this
553 result suggests that different neuronal elements in the SEG coordinate leg activity in a
554 complex, and not necessarily consistent, manner.

The synergy of leg CPGs, higher motor centers, and sensory information in walking

Walking behavior is dependent on the synergies of CPGs activities, sensory inputs, and higher motor center regulation. Our results indicate the SEG as a potential integration center: receiving descending inputs from the brain, as the anatomy of its neurons and those of the brain suggests (Roth et al., 1994), and ascending information from both leg sensory organs (Kien and Altman, 1984) and the CPGs themselves, as presented here.

Since we did not observe in any of our *in-vitro* experiments fictive walking, namely, a motor output that resembled a functional walking gait, we have to conclude that, in the locust, functional inter-leg coordination during walking is only accomplished by way of complementary sensory inputs or descending commands from the brain. This was also reported for many other walking systems (Büschges et al., 2011) and vast evidence suggests that sensory inputs plays a major role in walking coordination (e.g. Borgmann et al., 2007, 2009; Daun-Gruhn, 2011; Fuchs et al., 2012).

We did, however, find that the SEG affects the overall leg CPG coordination. Büschges et al. (1995; based on v. Holst, 1936) suggested that synchronized activity of locomotive oscillators is the energetically cheapest way to couple them while ensuring their joint frequency. As we have previously shown, the bilateral coupling among the CPGs in the thoracic ganglia is flexible and rather weak compared to the ipsilateral coupling (Knebel et al., 2017). It is therefore plausible that the level of bilateral synchronization mediated by the SEG is sufficient to drive the two ipsilateral trios of CPGs to oscillate at similar frequencies, as required for walking straight for example. Previous studies have already suggested that the SEG is a bilateral mediator (Kien and Altman, 1984; Kien et al., 1990; Bräunig and Burrows, 2004), but this was posited mostly due to the anatomy of the majority of the DIN branches, which are contralateral to their soma (Gal and Libersat, 2006). In light of this known DINs anatomy, and our physiological findings, it is plausible that a decussation of information and commands occurs in the SEG: ascending information about the CPGs activity and leg sensory inputs is received ipsilaterally, while the DINs deliver commands downstream via the contralateral descending axons, thus regulating the bilateral CPGs connections.

A comparison to vertebrate systems

A comparison of the anatomy and function of the SEG and the vertebrate brainstem suggests some parallels, as previously suggested by Schoofs et al. (2014). In the hindbrain-lesioned tadpole, for example, only short fictive swimming episodes could be elicited in response to tactile stimulus (Li et al., 2006), similar to the short sequences of walking that SEG-less insects perform (Gal and Libersat, 2006). Furthermore, subpopulations of brainstem neurons mapped functionally and anatomically were shown to be involved in locomotion initiation and halt (Shik et al., 1969; McClellan and Grillner, 1984; Sirota et al., 2000; Cabelguen et al., 2003; Hägglund et al., 2010; Esposito et al., 2014; Bouvier et al., 2015). Specifically, in all the different species examined, stimulation of the mesencephalic locomotor region (MLR) induced locomotion-related activity both *in-vivo* and *in-vitro* (Esposito and Arber, 2016). In the tadpole, neuronal pacemakers in the hindbrain that send descending neurites to the swimming CPGs fire at the beginning of each swimming cycle, presumably thereby maintaining a swimming pattern (Soffe et al., 2009). Our experiments showed that the SEG can elicit several burst cycles in the different leg depressors. It is therefore possible that, in a similar manner to the tadpole hindbrain, repetitive activity of SEG DINs at the appropriate time during the step cycle can excite the CPGs to be entrained in a functional manner.

Certain findings have also suggested that the brainstem mediates activity of both sides of the vertebrate body, analogically to the role of the SEG reported here. Each of the two-sided MLRs is capable of eliciting bilateral activation of the locomotion circuits along the spinal cord by activating both sides of the reticulospinal tracts simultaneously, thus delivering symmetrical commands to the spinal cord (Brocard et al., 2010). Furthermore, it is within the medulla oblongata that the pyramidal tracts (which include the motor corticospinal fibers), intersect to deliver information to the contralateral lower motor neurons. Moreover, similar to the brainstem, out of which the cranial nerves emerge, the SEG control the insect's mouthparts.

Conclusion

The SEG plays a regulative role in control of the arthropod legs. It has the ability to induce movement in all legs in different coordination patterns by activating their CPGs,

and it mediates their bilateral activity by adjusting the CPG coupling. Our findings have revealed ways by which the SEG higher motor center serves as a higher motor center of legged activity, as has been suggested in previous studies (Kien, 1983; Gal and Libersat, 2006; Bidaye et al., 2014). Overall, we show that the SEG interacts with the leg CPGs to organize their joint activity; and, being situated in-between the brain and thorax, it bridges between the brain centers, sensory inputs, and the motor circuits of the legs. Interestingly, a comparison between the SEG and the vertebrate brain stem suggests some parallels.

As noted above, findings based on *in-vitro* preparations are sometimes difficult to interpret, especially when they do not completely correspond to the real behavior. However, our findings did reveal functional connections between the leg CPGs and the SEG. Hence, the importance of the results, for understanding walking behavior, is clear. In light of the current findings and those of our previous study (Knebel et al., 2017), it is now known that the locust CPGs, with and without the SEG inputs, are not naturally coupled to produce any walking-like coordination. This is a consequence of the highly modulated system that has to adjust to the heterogeneous environment in which walking occurs, and therefore must avoid predetermined deterministic movements. Future work should explore the effects and the roles of other mechanisms modulating the CPG network, such as further higher motor centers and sensory inputs, and assess their contribution to walking.

References

Ayali A, Lange AB. 2010. Rhythmic behaviour and pattern-generating circuits in the locust: key concepts and recent updates. J Insect Physiol [Internet] 56:834–843. Available from: http://www.ncbi.nlm.nih.gov/pubmed/20303972

Ayali A, Zilberstein Y. 2002. The locust frontal ganglion: a multi-tasked central pattern generator. Acta Biol Hung 55:129–135.

Bal T, Nagy F, Moulins M. 1988. The pyloric central pattern generator in Crustacea: a set of conditional neuronal oscillators. J Comp Physiol A 163:715–727.

Bässler U. 1983. Neural Basis of Elementary Behavior in Stick Insects. Berlin, Heidelberg: Springer Berlin Heidelberg. Available from: http://link.springer.com/10.1007/978-3-642-68813-3

Bässler U, Foth E, Breutel G. 1985. The inherent walking direction differs for the prothoracic and metathoracic legs of stick insects. J Exp Biol [Internet] 116:301–311. Available from: http://jeb.biologists.org/content/116/1/301.short

649 Bender JA, Pollack AJ, Ritzmann RE. 2010. Neural Activity in the Central Complex of
650 the Insect Brain Is Linked to Locomotor Changes. Curr Biol [Internet] 20:921–926.
651 Available from: http://www.ncbi.nlm.nih.gov/pubmed/20451382
652 Berkowitz A, Laurent G. 1996. Central generation of grooming motor patterns and
653 interlimb coordination in locusts. J Neurosci 16:8079–8091.
654 Bidaye SS, Machacek C, Wu Y, Dickson BJ. 2014. Neuronal Control of Drosophila
655 Walking Direction. Science [Internet] 344:97–101. Available from:
656 http://www.sciencemag.org/cgi/doi/10.1126/science.1249964
657 Borgmann A, Hooper SL, Büschges A. 2009. Sensory feedback induced by front-leg
658 stepping entrains the activity of central pattern generators in caudal segments of the
659 stick insect walking system. J Neurosci [Internet] 29:2972–2983. Available from:
660 http://www.ncbi.nlm.nih.gov/pubmed/19261892
661 Borgmann A, Scharstein H, Büschges A. 2007. Intersegmental coordination: influence of
662 a single walking leg on the neighboring segments in the stick insect walking system.
663 J Neurophysiol [Internet] 98:1685–1696. Available from:
664 http://www.ncbi.nlm.nih.gov/pubmed/17596420
665 Bouvier J, Caggiano V, Leiras R, Caldeira V, Bellardita C, Balueva K, Fuchs A, Kiehn
666 O. 2015. Descending Command Neurons in the Brainstem that Halt Locomotion.
667 Cell [Internet] 163:1191–1203. Available from:
668 http://dx.doi.org/10.1016/j.cell.2015.10.074
669 Bräunig P. 1991. Suboesophageal DUM Neurons Innervate the Principal Neuropiles of
670 the Locust Brain. Philos Trans R Soc B Biol Sci [Internet] 332:221–240. Available
671 from: http://rstb.royalsocietypublishing.org/cgi/doi/10.1098/rstb.1991.0051
672 Bräunig P, Burrows M. 2004. Projection patterns of posterior dorsal unpaired median
673 neurons of the locust subesophageal ganglion. J Comp Neurol 478:164–175.
674 Brocard F, Ryczko D, Fenelon K, Hatem R, Gonzales D, Auclair F, Dubuc R. 2010. The
675 transformation of a unilateral locomotor command into a symmetrical bilateral
676 activation in the brainstem. J Neurosci [Internet] 30:523–533. Available from:
677 http://www.ncbi.nlm.nih.gov/pubmed/20071515
678 Büschges A, Schmitz J, Bässler U. 1995. Rhythmic patterns in the thoracic nerve cord of
679 the stick insect induced by pilocarpine. J Exp Biol [Internet] 198:435–456.
680 Available from: http://www.ncbi.nlm.nih.gov/pubmed/9318078
681 Büschges A, Scholz H, El Manira A. 2011. New moves in motor control. Curr Biol
682 [Internet] 21:R513–R524. Available from:
683 http://www.ncbi.nlm.nih.gov/pubmed/21741590
684 Cabelguen J-M, Bourcier-Lucas C, Dubuc R. 2003. Bimodal locomotion elicited by
685 electrical stimulation of the midbrain in the salamander Notophthalmus viridescens.
686 J Neurosci 23:2434–2439.
687 Campbell JI. 1961. The anatomy of the nervous system of the mesothorax of Locusta
688 migratoria migradorioides R. & F. In: Proceedings of the Zoological Society of
689 London. Vol. 137. Wiley Online Library. p 403–432.
690 Cholewa J, Pflüger H-J. 2009. Descending unpaired median neurons with bilaterally
691 symmetrical axons in the suboesophageal ganglion of Manduca sexta larvae.
692 Zoology (Jena) [Internet] 112:251–262. Available from:
693 http://www.ncbi.nlm.nih.gov/pubmed/19423308
694 Chrachri A, Clarac F. 1987. Induction of rhythmic activity in motoneurons of crayfish

thoracic ganglia by cholinergic agonists. Neurosci Lett 77:49–54.

Daun-Gruhn S. 2011. A mathematical modeling study of inter-segmental coordination during stick insect walking. J Comput Neurosci [Internet] 30:255–278. Available from: http://www.ncbi.nlm.nih.gov/pubmed/20567889

David I, Holmes P, Ayali A. 2016. Endogenous rhythm and pattern-generating circuit interactions in cockroach motor centres. Biol Open [Internet] 5:1229–1240. Available from: http://www.ncbi.nlm.nih.gov/pubmed/27422902

Dubuc R, Brocard F, Antri M, Fénelon K, Gariépy J-F, Smetana R, Ménard A, Le Ray D, Viana Di Prisco G, Pearlstein E, Sirota MG, Derjean D, St-Pierre M, Zielinski B, Auclair F, Veilleux D. 2008. Initiation of locomotion in lampreys. Brain Res Rev [Internet] 57:172–182. Available from: http://www.ncbi.nlm.nih.gov/pubmed/17916380

Esposito MS, Arber S. 2016. Motor Control: Illuminating an Enigmatic Midbrain Locomotor Center. Curr Biol [Internet] 26:R291–R293. Available from: http://dx.doi.org/10.1016/j.cub.2016.02.043

Esposito MS, Capelli P, Arber S. 2014. Brainstem nucleus MdV mediates skilled forelimb motor tasks. Nature [Internet] 508:351–356. Available from: http://www.ncbi.nlm.nih.gov/pubmed/24487621

Fritsch G, Hitzig E. 2009. Electric excitability of the cerebrum (Über die elektrische Erregbarkeit des Grosshirns). Epilepsy Behav [Internet] 15:123–130. Available from: http://linkinghub.elsevier.com/retrieve/pii/S1525505009001334

Fuchs E, Holmes P, David I, Ayali A. 2012. Proprioceptive feedback reinforces centrally generated stepping patterns in the cockroach. J Exp Biol [Internet] 215:1884–1891. Available from: http://www.ncbi.nlm.nih.gov/pubmed/22573767

Fuchs E, Holmes P, Kiemel T, Ayali A. 2011. Intersegmental coordination of cockroach locomotion: adaptive control of centrally coupled pattern generator circuits. Front Neural Circuits [Internet] 4:125. Available from: http://www.pubmedcentral.nih.gov/articlerender.fcgi?artid=3043608&tool=pmcentrez&rendertype=abstract

Gal R, Libersat F. 2006. New vistas on the initiation and maintenance of insect motor behaviors revealed by specific lesions of the head ganglia. J Comp Physiol A Neuroethol Sensory, Neural, Behav Physiol [Internet] 192:1003–1020. Available from: http://www.ncbi.nlm.nih.gov/pubmed/16733727

Gal R, Libersat F. 2008. A Parasitoid Wasp Manipulates the Drive for Walking of Its Cockroach Prey. Curr Biol [Internet] 18:877–882. Available from: http://www.pubmedcentral.nih.gov/articlerender.fcgi?artid=2850919&tool=pmcentrez&rendertype=abstract

Gordon IT, Whelan PJ. 2008. Brainstem modulation of locomotion in the neonatal mouse spinal cord. J Physiol [Internet] 586:2487–2497. Available from: http://doi.wiley.com/10.1113/jphysiol.2007.148320

Grabowska M, Godlewska E, Schmidt J, Daun-Gruhn S. 2012. Quadrupedal gaits in hexapod animals - inter-leg coordination in free-walking adult stick insects. J Exp Biol [Internet] 215:4255–4266. Available from: http://www.ncbi.nlm.nih.gov/pubmed/22972892

Gray JR, Robertson RM. 1998. Effects of heat stress on axonal conduction in the locust flight system. Comp Biochem Physiol Part A Mol Integr Physiol [Internet] 120:181–

741 186. Available from:
742 http://linkinghub.elsevier.com/retrieve/pii/S1095643398100284
743 Hägglund M, Borgius L, Dougherty KJ, Kiehn O. 2010. Activation of groups of
744 excitatory neurons in the mammalian spinal cord or hindbrain evokes locomotion.
745 Nat Neurosci [Internet] 13:246–52. Available from:
746 http://www.ncbi.nlm.nih.gov/pubmed/20081850
747 Heidel E, Pflüger HJ. 2006. Ion currents and spiking properties of identified subtypes of
748 locust octopaminergic dorsal unpaired median neurons. Eur J Neurosci 23:1189–
749 1206.
750 v. Holst E. 1936. Über den „Magnet-Effekt“ als koordinierendes Prinzip im Rückenmark.
751 Pflüger’s Arch für die gesamte Physiol des Menschen und der Tiere [Internet]
752 237:655–682. Available from: http://link.springer.com/10.1007/BF01753051
753 Huber F. 1960. Untersuchungen über die Funktion des Zentralnervensystems und
754 insbesondere des Gehirnes bei der Fortbewegung und der Lauterzeugung der
755 Grillen. Z Vgl Physiol 44:60–132.
756 Hussaini SA, Menzel R. 2013. Mushroom Body Extrinsic Neurons in the Honeybee
757 Brain Encode Cues and Contexts Differently. J Neurosci [Internet] 33:7154–7164.
758 Available from: http://www.jneurosci.org/cgi/doi/10.1523/JNEUROSCI.1331-
759 12.2013
760 Ito K, Shinomiya K, Ito M, Armstrong JD, Boyan G, Hartenstein V, Harzsch S,
761 Heisenberg M, Homberg U, Jenett A, Keshishian H, Restifo LL, Roessler W,
762 Simpson JH, Strausfeld NJ, Strauss R, Vosshall LB. 2014. A systematic
763 nomenclature for the insect brain. Neuron 81:755–765.
764 Jeannerod M, Arbib M. 2003. Action monitoring and forward control of movements. In:
765 Arbib M, editor. The Handbook of Brain Theory and Neural Networks. 2nd ed.
766 Cambridge, MA: MIT Press. p 83–85.
767 Johnston RM, Levine RB. 2002. Thoracic leg motoneurons in the isolated CNS of adult
768 Manduca produce patterned activity in response to pilocarpine, which is distinct
769 from that produced in larvae. Invertebr Neurosci 4:175–192.
770 Kahn J, Roberts A. 1982a. The central nervous origin of the swimming motor pattern in
771 embryos of Xenopus Laevis. J Exp Biol [Internet] 99:185–196. Available from:
772 http://www.ncbi.nlm.nih.gov/pubmed/7130897
773 Kahn J, Roberts A. 1982b. Experiments on the Central Pattern Generator for Swimming
774 in Amphibian Embryos. Philos Trans R Soc B Biol Sci [Internet] 296:229–243.
775 Available from:
776 http://rstb.royalsocietypublishing.org/cgi/doi/10.1098/rstb.1982.0004
777 Kaiser M, Libersat F. 2015. The role of the cerebral ganglia in the venom-induced
778 behavioral manipulation of cockroaches stung by the parasitoid jewel wasp. J Exp
779 Biol 218:1022–1027.
780 Kien J. 1983. The Initiation and Maintenance of Walking in the Locust: An Alternative to
781 the Command Concept. Proc R Soc B Biol Sci [Internet] 219:137–174. Available
782 from: http://rspb.royalsocietypublishing.org/cgi/doi/10.1098/rspb.1983.0065
783 Kien J. 1990a. Neuronal activity during spontaneous walking-I. Starting and stopping.
784 Comp Biochem Physiol -- Part A Physiol [Internet] 95:607–621. Available from:
785 http://www.sciencedirect.com/science/article/pii/030096299090747G
786 Kien J. 1990b. Neuronal activity during spontaneous walking--II. Correlation with

787 stepping. Comp Biochem Physiol Part A [Internet] 95:623–638. Available from:
788 http://www.ncbi.nlm.nih.gov/pubmed/1971548
789 Kien J, Altman JS. 1984. Descending interneurones from the brain and suboesophageal
790 ganglia and their role in the control of locust behaviour. J Insect Physiol [Internet]
791 30:59–72. Available from:
792 http://www.sciencedirect.com/science/article/pii/0022191084901082
793 Kien J, Altman JS. 1992. Preparation and execution of movement: parallels between
794 insect and mammalian motor systems. Comp Biochem Physiol Comp Physiol
795 [Internet] 103:15–24. Available from:
796 http://www.ncbi.nlm.nih.gov/pubmed/1356693
797 Kien J, Fletcher WA, Altman JS, Ramirez JM, Roth U. 1990. Organisation of
798 intersegmental interneurons in the suboesophageal ganglion of Schistocerca gregaria
799 (Forksal) and Locusta migratoria migratorioides (Reiche & Fairmaire) (Acrididae,
800 Orthoptera. Int J Insect Morphol Embryol [Internet] 19:35–60. Available from:
801 http://linkinghub.elsevier.com/retrieve/pii/002073229090029O
802 Kien J, Williams M. 1983. Morphology of Neurons in Locust Brain and Suboesphageal
803 Ganglion Involved in Initiation and Maintenance of Walking. Proc R Soc B Biol Sci
804 [Internet] 219:175–192. Available from:
805 http://rspb.royalsocietypublishing.org/cgi/doi/10.1098/rspb.1983.0066
806 Knebel D, Ayali A, Pflueger H-J, Rillich J. 2017. Rigidity and Flexibility: The Central
807 Basis of Inter-Leg Coordination in the Locust. Front Neural Circuits 10:112.
808 Li WC, Roberts A, Soffe SR. 2009. Locomotor rhythm maintenance: electrical coupling
809 among premotor excitatory interneurons in the brainstem and spinal cord of young
810 Xenopus tadpoles. J Physiol [Internet] 587:1677–1693. Available from:
811 http://www.pubmedcentral.nih.gov/articlerender.fcgi?artid=2683956&tool=pmcentr
812 ez&rendertype=abstract
813 Li WC, Roberts A, Soffe SR. 2010. Specific brainstem neurons switch each other into
814 pacemaker mode to drive movement by activating NMDA receptors. J Neurosci
815 [Internet] 30:16609–16620. Available from:
816 http://www.pubmedcentral.nih.gov/articlerender.fcgi?artid=3044868&tool=pmcentr
817 ez&rendertype=abstract
818 Li WC, Soffe SR, Wolf E, Roberts A. 2006. Persistent responses to brief stimuli:
819 feedback excitation among brainstem neurons. J Neurosci [Internet] 26:4026–4035.
820 Available from: http://www.ncbi.nlm.nih.gov/pubmed/16611819
821 Libersat F, Pflueger H-J. 2004. Monoamines and the Orchestration of Behavior.
822 Bioscience 54:17–25.
823 Marder E. 2012. Neuromodulation of Neuronal Circuits: Back to the Future. Neuron
824 [Internet] 76:1–11. Available from: http://dx.doi.org/10.1016/j.neuron.2012.09.010
825 Marder E, Bucher D. 2001. Central pattern generators and the control of rhythmic
826 movements. Curr Biol [Internet] 11:R986–R996. Available from:
827 http://www.ncbi.nlm.nih.gov/pubmed/11728329
828 Marder E, Bucher D. 2007. Understanding circuit dynamics using the stomatogastric
829 nervous system of lobsters and crabs. Annu Rev Physiol 69:291–316.
830 McClellan AD, Grillner S. 1984. Activation of “fictive swimming” by electrical
831 microstimulation of brainstem locomotor regions in an in vitro preparation of the
832 lamprey central nervous system. Brain Res [Internet] 300:357–361. Available from:

http://www.ncbi.nlm.nih.gov/pubmed/6733478

Miller WL, Sigvardt KA. 1998. Spectral analysis of oscillatory neural circuits. J Neurosci Methods 80:113–128.

Mu L, Ritzmann RE. 2008. Interaction between descending input and thoracic reflexes for joint coordination in cockroach: I. Descending influence on thoracic sensory reflexes. J Comp Physiol A Neuroethol Sensory, Neural, Behav Physiol [Internet] 194:283–298. Available from: http://www.ncbi.nlm.nih.gov/pubmed/18094976

Mulloney B, Smarandache C. 2010. Fifty Years of CPGs: Two Neuroethological Papers that Shaped the Course of Neuroscience. Front Behav Neurosci [Internet] 4:1–8. Available from: http://www.pubmedcentral.nih.gov/articlerender.fcgi?artid=2917247&tool=pmcentrez&rendertype=abstract

Penfield W, Boldrey E. 1937. Somatic motor and sensory representation in the cerebral cortex of man as studied by electrical stimulation. Brain A J Neurol 60:389–443.

Pfeiffer K, Homberg U. 2014. Organization and functional roles of the central complex in the insect brain. Annu Rev Entomol [Internet] 59:165–84. Available from: http://www.ncbi.nlm.nih.gov/pubmed/24160424

Poeck B, Triphan T, Neuser K, Strauss R. 2008. Locomotor control by the central complex in Drosophila - An analysis of the tay bridge mutant. Dev Neurobiol [Internet] 68:1046–1058. Available from: http://www.ncbi.nlm.nih.gov/pubmed/18446784

Rand D, Knebel D, Ayali A. 2012. The effect of octopamine on the locust stomatogastric nervous system. Front Physiol [Internet] 3:288. Available from: http://www.pubmedcentral.nih.gov/articlerender.fcgi?artid=3429060&tool=pmcentrez&rendertype=abstract

Ridgel AL, Ritzmann RE. 2005. Effects of neck and circumoesophageal connective lesions on posture and locomotion in the cockroach. J Comp Physiol A 191:559–573.

Rillich J, Stevenson PA, Pflüger H-J. 2013. Flight and Walking in Locusts-Cholinergic Co-Activation, Temporal Coupling and Its Modulation by Biogenic Amines. PLoS One [Internet] 8:e62899. Available from: http://www.pubmedcentral.nih.gov/articlerender.fcgi?artid=3650027&tool=pmcentrez&rendertype=abstract

Roth U, Kien J, Altman JS. 1994. Projections of suboesophageal descending interneurons in thoracic ganglia of the grasshopper Omocestus viridulus L. (Orthoptera: Acrididae). Int J Insect Morphol Embryol [Internet] 23:275–291. Available from: http://www.sciencedirect.com/science/article/pii/0020732294900248

Rybak IA, Dougherty KJ, Shevtsova NA. 2015. Organization of the Mammalian Locomotor CPG: Review of Computational Model and Circuit Architectures Based on Genetically Identified Spinal Interneurons. eNeuro [Internet] 2. Available from: http://eneuro.sfn.org/cgi/doi/10.1523/ENEURO.0069-15.2015

Ryckebusch S, Laurent G. 1993. Rhythmic patterns evoked in locust leg motor neurons by the muscarinic agonist pilocarpine. J Neurophysiol [Internet] 69:1583–1595. Available from: http://www.ncbi.nlm.nih.gov/pubmed/8389831

Ryckebusch S, Laurent G. 1994. Interactions between segmental leg central pattern generators during fictive rhythms in the locust. J Neurophysiol [Internet] 72:2771–

2785. Available from: http://www.ncbi.nlm.nih.gov/pubmed/7897488

Ryckebusch S, Wehr M, Laurent G. 1994. Distinct rhythmic locomotor patterns can be generated by a simple adaptive neural circuit: Biology, simulation, and VLSI implementation. J Comput Neurosci [Internet] 1:339–358. Available from: http://www.ncbi.nlm.nih.gov/pubmed/8792239

Schmidt RA, Lee TD. 2005. Motor Control and Learning: A Behaviour Emphasis. 5th ed. Champaign, IL: Human kinetics.

Schoofs A, Hückesfeld S, Schlegel P, Miroschnikow A, Peters M, Zeymer M, Spieß R, Chiang AS, Pankratz MJ. 2014. Selection of Motor Programs for Suppressing Food Intake and Inducing Locomotion in the Drosophila Brain. PLoS Biol 12.

Shik ML, Severin F V, Orlovsky GN. 1969. Control of walking and running by means of electrical stimulation of the mesencephalon. Electroencephalogr Clin Neurophysiol [Internet] 26:549. Available from: http://www.ncbi.nlm.nih.gov/pubmed/4181500

Sigvardt KA, Miller WL. 1998. Analysis and modeling of the locomotor central pattern generator as a network of coupled oscillators. In: Annals of the New York Academy of Sciences. Vol. 860. . p 250–265.

Sirota MG, Di Prisco GV, Dubuc R. 2000. Stimulation of the mesencephalic locomotor region elicits controlled swimming in semi-intact lampreys. Eur J Neurosci 12:4081–4092.

Soffe SR, Roberts A, Li WC. 2009. Defining the excitatory neurons that drive the locomotor rhythm in a simple vertebrate: insights into the origin of reticulospinal control. J Physiol [Internet] 587:4829–4844. Available from: http://www.pubmedcentral.nih.gov/articlerender.fcgi?artid=2770150&tool=pmcentrez&rendertype=abstract

Stevenson PA, Kutsch W. 1987. A reconsideration of the central pattern generator concept for locust flight. J Comp Physiol A [Internet] 161:115–129. Available from: http://link.springer.com/10.1007/BF00609460

Stevenson PA, Sporhase-Eichmann U. 1995. Localization of octopaminergic neurons in insects. Comp Biochem Physiol B 11:203–215.

Strausfeld NJ, Hansen L, Li Y, Gomez RS, Ito K. 1998. Evolution, discovery, and interpretations of arthropod mushroom bodies. Learn Mem [Internet] 5:11–37. Available from: http://www.ncbi.nlm.nih.gov/pubmed/10454370

Strauss R. 2002. The central complex and the genetic dissection of locomotor behaviour. Curr Opin Neurobiol [Internet] 12:633–638. Available from: http://linkinghub.elsevier.com/retrieve/pii/S0959438802003859

Tastekin I, Riedl J, Schilling-Kurz V, Gomez-Marin A, Truman JW, Louis M. 2015. Role of the subesophageal zone in sensorimotor control of orientation in drosophila larva. Curr Biol [Internet] 25:1448–1460. Available from: http://dx.doi.org/10.1016/j.cub.2015.04.016

Wilson M. 1966. Insect Walking. Annu Rev Entomol [Internet]:103–122. Available from: http://www.annualreviews.org/doi/pdf/10.1146/annurev.en.11.010166.000535

Legends

Figure 1

SEG electrical stimulation elicits leg motor outputs. (A) Scan of the SEG after staining one neck connective. The dyed somas represent about half of the SEG DIN population. Scale bar: 100 µm **(B)** Maximum intensity projection showing the double labeling of neck connective (red) and nerve 5A staining (green) in the metathoracic ganglion. Arrows in the pictograms and the scan indicate the stained nerves. Scale bar: 100 µm. **(C)** A single horizontal optical section from the framed zone in **(B)**, showing the overlapping area of the depressor motor neurons and DINs projections. Scale bar:100 µm **(D)** An example of a typical SEG stimulation of the neurons of the mandibular neuromere resulting in a brief elicited activity of the depressor MN of the pro- and mesothoracic ganglia. Scale bar: 5 s **(E)** An example of a typical SEG stimulation of the labial neuromere resulting in a prolonged rhythmic bursting activity of all recorded thoracic ganglia (Df, fast depressor; Ds, slow depressor; CI, common inhibitor). Scale bar: 5 s.

Figure 2

Pharmacological stimulation of the metathoracic ganglion induces rhythmic bursting activity in all three thoracic ganglia. (A) The pictogram schematically presents the three thoracic ganglia and SEG. Pilocarpine was applied to the metathoracic ganglion only, as indicated by the gray filling. The arrows indicate the recording sites (4 depressor nerves and 3 connectives), as demonstrated by the recording trace. Scale bar:10 s. **(B)** The spike frequency throughout the 8 min of recording, for each hemiganglion (pro-, meso-, metathoracic hemigagnlia – T1, T2 and T3, respectively), with and without the SEG. No significant difference was found. **(C)** The most common frequency of the pro- and mesothoracic hemiganglia and the ipsilateral source of activation – the ipsilateral hemiganglia (T1 and T2, respectively), before and after SEG removal. Again, no significant difference was found.

Figure 3

The overall CPG-CPG phase relations are affected by the SEG. (A) The bilateral synchrony of the prothoracic CPGs before the SEG removal. The recording exemplifies the typical bursting activity of both hemiganglia. The circular histogram presents the phase of the prothoracic contralateral CPGs of all experiments. The bar filling colors represents the value of the synchronization index, as indicated by the color scale below. The sample size represents only the experiments in which we recorded the bilateral prothoracic activity. **(B)** As in **(A)** but for the activity of prothoracic CPGs after the SEG removal. The phase calculated for the two conditions was significantly different. Scale bar: 2 s. **(C)** A scheme of the CPGs phases before the SEG removal. The colors of the interconnecting lines between the pro-, meso- and metathoracic hemiganglia (upper, middle, and bottom circle pairs, respectively), represent the synchronization index values of each pair of CPGs, as shown on the color scale on the right. **(D)** As in **(C)** but after the SEG removal. **(E)** As in **(C)** but for experiments in which the SEG was removed from the thoracic ganglia chain at the dissection stage. Note that after the SEG removal, the bilateral CPG connections are drawn to anti-phase activity, while the ipsilateral connections remain in-phase, similarly to the experiments in which the SEG was not present from the beginning. *** $p<0.001$.

Figure 4

SEG interneurons activity correlates with the prothoracic depressors joint activity. (A) Overlays of three simultaneous recordings from the connectives (one for each), indicated by the arrows in the pictogram. The black line represents the average vector of these overlays. The constant delay of 1.8 ms from the SEG downwards to the ipsilateral pro-meso connective indicates that the spike is generated by a neuron in the SEG, sending a descending neurite to all thoracic ganglia. Scale bar: 5 ms **(B)** Cross-covariance between the SEG DIN firing and the left and right prothoracic depressors (blue and red lines, respectively) and the right metathoracic depressor (green line). **(C)** Cross-covariance between the left and right prothoracic CPGs. **(D)** Merged cross-covariance of the left and right prothoracic depressors with the SEG DIN, from the narrow grayed window in **(B)**. The intersection of the 0 values presents the time of the SEG DIN firing, and the colors indicate degree of correlation between the left and right depressors, as indicated by the color scale above. Note that the blue spot in **(D)** is smeared upwards, indicating that the peak of correlation is not at the spike onset, and a delayed prolonged elicited activity is recorded from the CPG contralateral to the DIN. Since no clear correlation is found between the DIN and the metathoracic depressor, as shown in **(B)**, it is a candidate DIN for specifically synchronizing the prothoracic contralateral CPGs. **(E)** Simultaneous intracellular recording of a SEG neuron and the thoracic motor activity. Horizontal and vertical scale bars: 1 s and 10 mV, respectively. The confocal scan shows the recorded SEG neuron. Note that the neuron sends a neurite to the neck connective (indicated by the white arrow). Scale bar:80 µm. **(F)** Cross-covariance between the SEG DIN membrane potential and the left and right prothoracic depressors (blue and red lines, respectively) and the right metathoracic depressor (green line). **(G)** As in (**C**), but for the prothoracic activity in the preparation shown in (**E**). **(H)** As in **(D)**, but for the prothoracic and DIN activity in this preparation shown in (**E**) Note the resemblance to the SEG DIN shown in (**D**). **(I)** Simultaneous intracellular recording of SEG neuron and the thoracic motor activity. Horizontal and vertical scale bars:1 s and 10 mV, respectively. The confocal scan shows the recorded SEG neuron. Scale bar: 80 µm. **(J)** Cross-covariance between the SEG interneuron spikes and the left and right prothoracic depressors (blue and red lines, respectively), and the right metathoracic depressor (green line). **(K)** As in (**C**), but for the prothoracic activity in the preparation shown in (**I**) **(L)** As in **(D)**, but for the prothoracic and DIN activity in this preparation shown in **(I**). Note that despite the weak correlation between the left and right depressors, as seen in **(K)**, the correlation at the time of the SEG neuron spike is clear, as seen in **(J)**.

Figure 5

A SEG DUM neuron activity is correlated with the prothoracic depressors joint activity. (A) An overlay of 3 recordings from the connectives, shown by the arrows in the pictogram. The almost simultaneous spike (constant delay of 0.4 ms) in both the left and right connectives indicates that the spike is generated by a neuron in the SEG, sending two descending neurites to the thoracic ganglia, typical for SEG DUM neurons. Scale bar: 5 ms. **(B)** Cross-covariance between the SEG DIN firing and the left and right prothoracic depressors (blue and red lines, respectively) and the right metathoracic

depressor (green line). **(C)** Cross-covariance between the left and right prothoracic CPGs. **(D)** Merged cross-covariance of the left and right prothoracic depressors with the SEG DIN, from the narrow grayed window in **(B)**. The intersection of the 0 values presents the time of the SEG DIN firing, and the colors indicate degree of correlation between the left and right depressors, as indicated by the color scale above.

Figure 6

A SEG DUM neuron activity is correlated with the prothoracic depressors joint activity. (A) Confocal scan shows the recorded SEG neuron. Scale bar: 80 µm. **(B)** Simultaneous intracellular recording of SEG neuron and the thoracic motor activity. Horizontal and vertical scale bars: 50 ms and 10 mV, respectively. Note the medial position of the neuron, its symmetrical arborization, and its long duration soma spikes. Together, these neuronal characteristics indicate that it is a SEG DUM neuron. **(C)** Cross-covariance between the SEG DIN firing and different sets of depressors (right prothoracic: blue; left prothoracic: red; right metathoracic: green). **(D)** Cross-covariance between the left and right prothoracic depressors **(E)** Merged cross-covariance of the left and right prothoracic depressors with the SEG DIN, from the narrow grayed window in **(C)**. The intersection of the 0 values presents the time of the SEG DIN firing, and the colors indicate degree of correlation between the left and right depressors, as indicated by the color scale above. **(F)** Simultaneous intracellular recording of SEG neuron and the thoracic motor activity before, during, and after a short depolarization. Horizontal and vertical scale bars: 2 s and 10 mV, respectively. **(G)** Simultaneous intracellular recording of the SEG DIN and the thoracic motor activity during a permanent hyperpolarization. Horizontal and vertical scale bars: 2 s and 10 mV, respectively. **(H)**, **(I)** and **(J)** are the same as **(C), (D),** & **(E)** respectively, but for the SEG DIN during the permanent hyperpolarization, and conducted by analyzing the changes in its membrane potential.

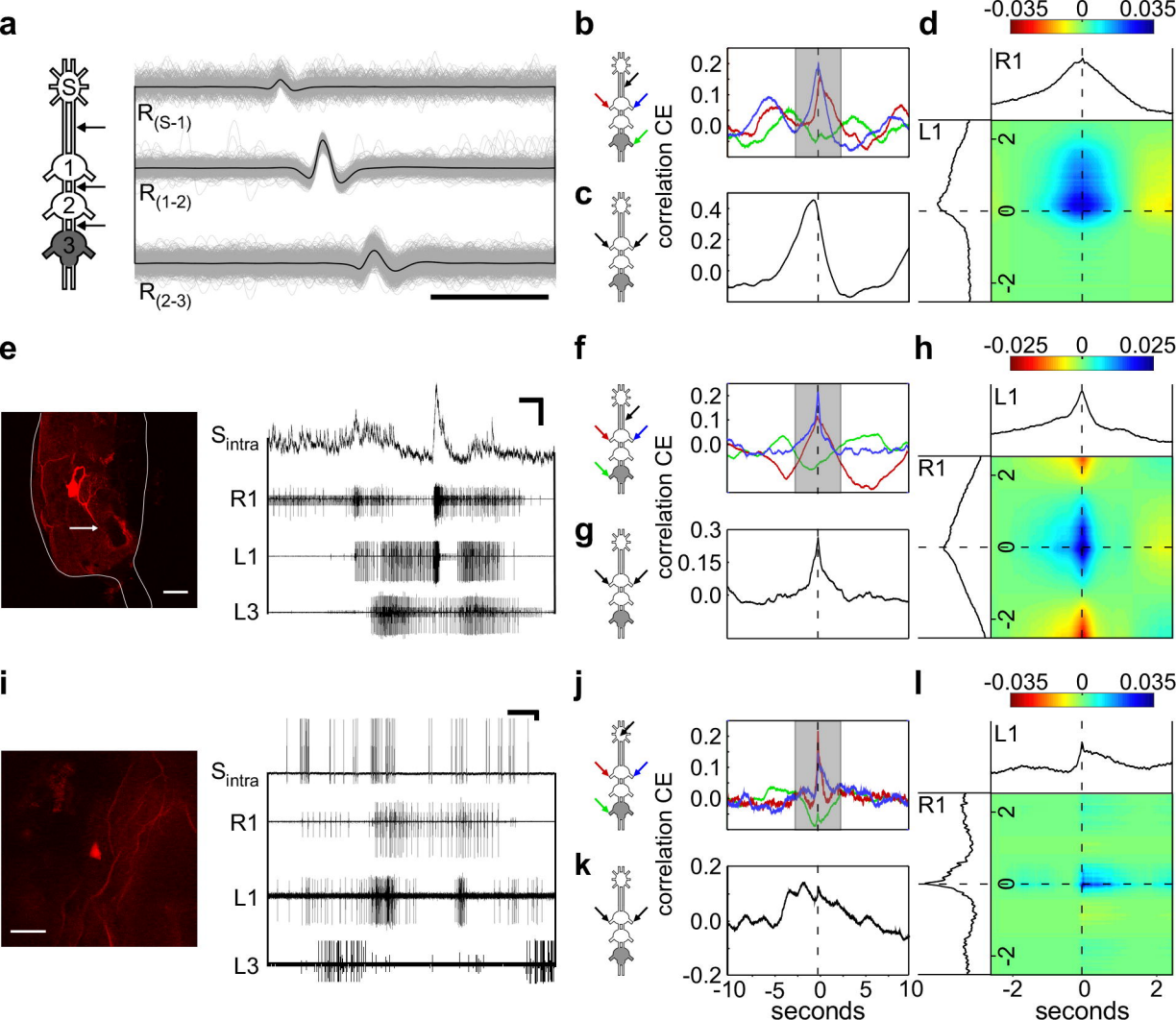
a
S
1
2
3
R(S-1)
R(1-2)
R(2-3)
b
c
correlation CE
0.2
0.1
0.0
0.4
0.2
0.0
d
-0.035
0
0.035
R1
L1
2
0
-2
e
Sintra
R1
L1
L3
f
g
0.3
0.15
0.0
h
-0.025
0.025
i
j
k
0.2
0.0
-0.2
-10
-5
0
5
10
seconds
l
-2
0
2

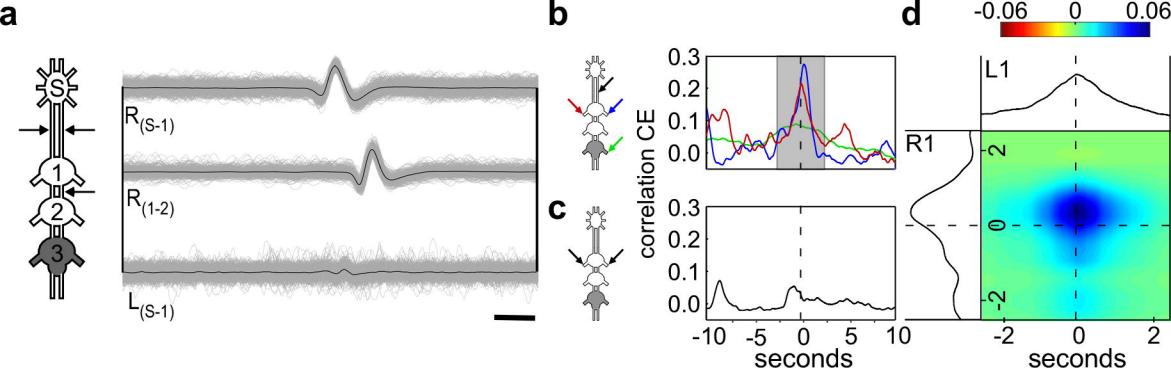
a
S
1
2
3
R(S-1)
R(1-2)
L(S-1)
b
c
correlation CE
0.3
0.2
0.1
0.0
-10 -5 0 5 10
seconds
d
-0.06 0 0.06
L1
R1
2
0
-2
-2 0 2
seconds

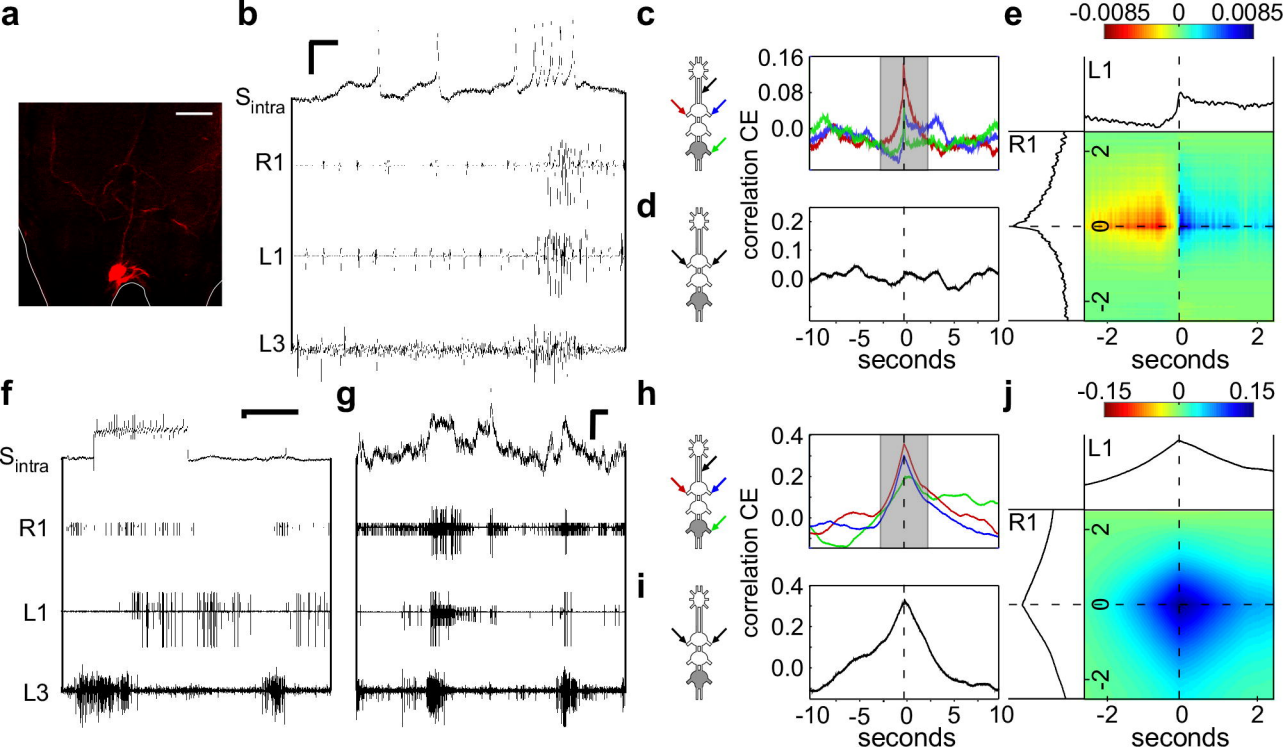
a
b
c
d
e
f
g
h
i
j
S intra
R1
L1
L3
correlation CE
seconds
-0.0085 0 0.0085
-0.15 0 0.15

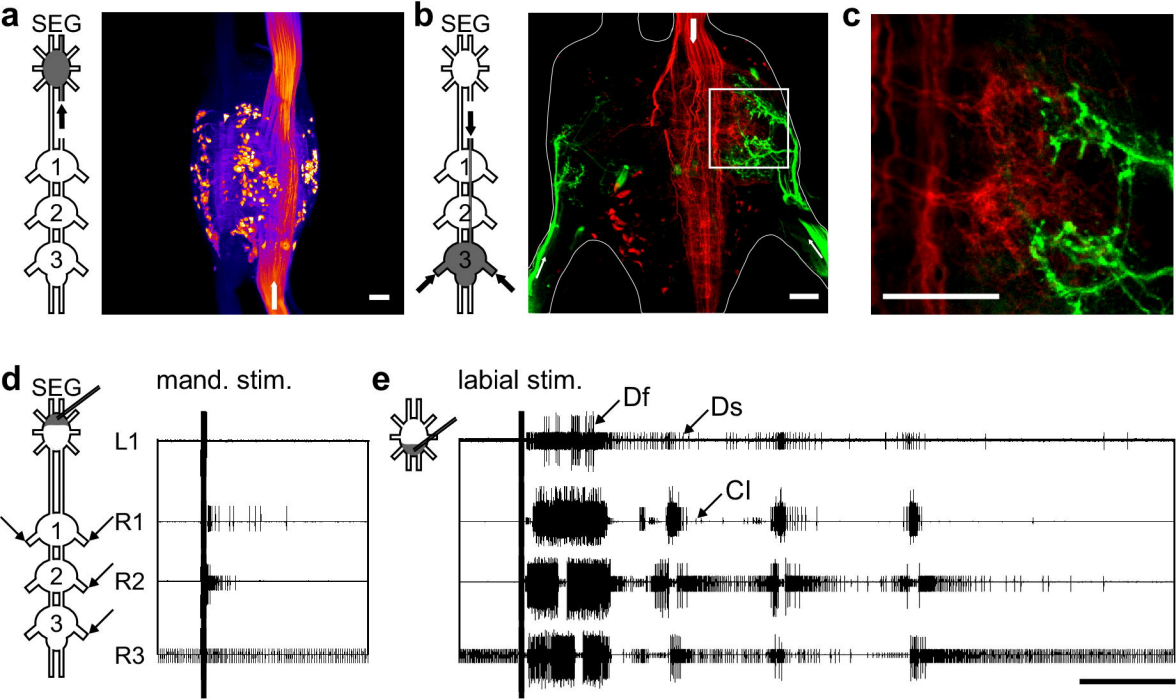
a
SEG
1
2
3
b
SEG
1
2
3
c
d
SEG
mand. stim.
L1
R1
R2
R3
1
2
3
e
labial stim.
Df
Ds
CI

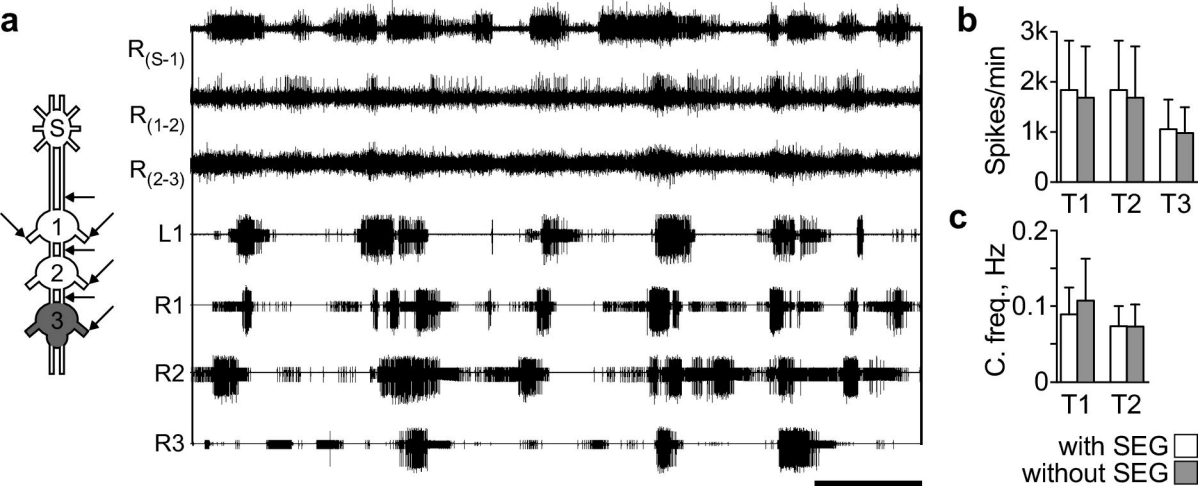
a
S
1
2
3
R(S-1)
R(1-2)
R(2-3)
L1
R1
R2
R3
b
Spikes/min
3k
2k
1k
0
T1
T2
T3
c
C. freq., Hz
0.2
0.1
0
T1
T2
with SEG
without SEG

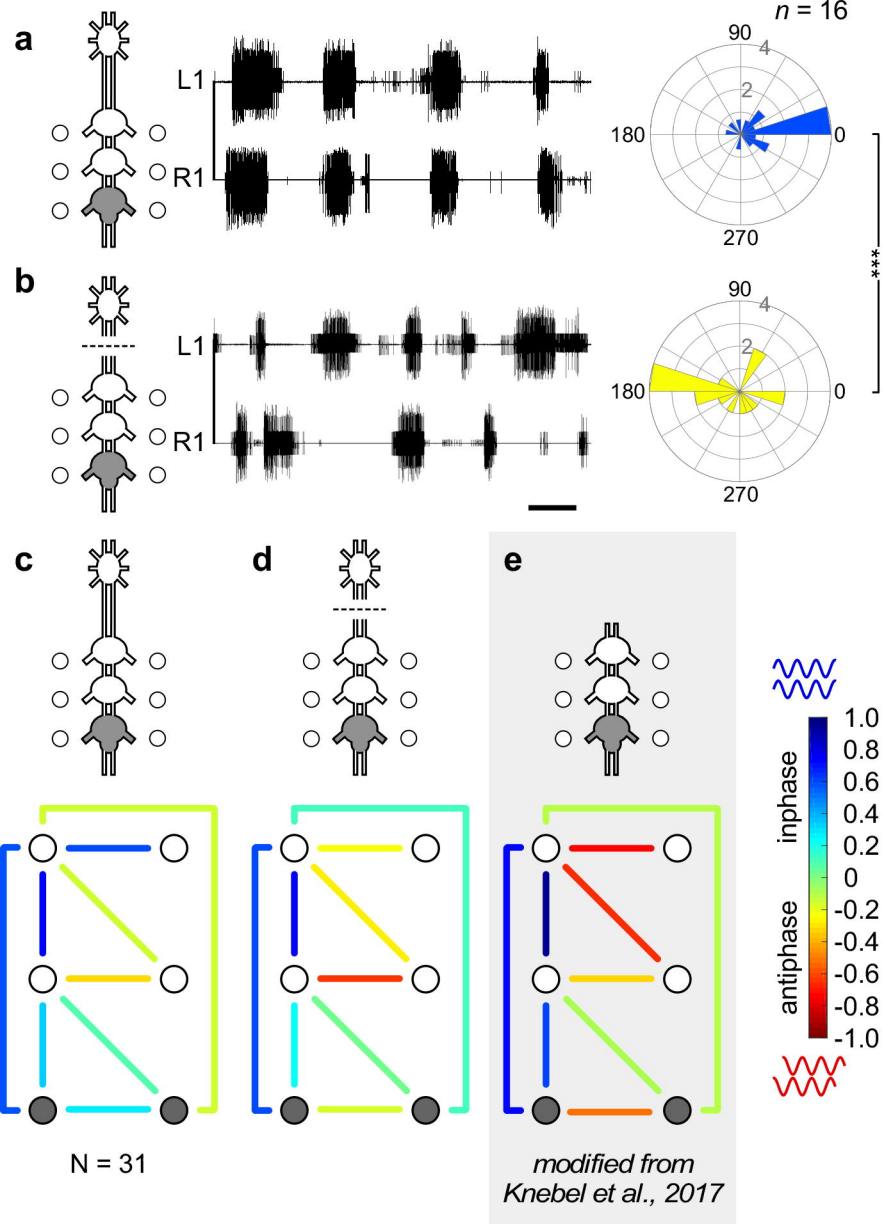
a
L1
R1
n = 16
90
4
2
180
0
270
***
b
L1
R1
90
4
2
180
0
270
c
d
e
1.0
0.8
0.6
0.4
0.2
0
-0.2
-0.4
-0.6
-0.8
-1.0
inphase
antiphase
N = 31
modified from
Knebel et al., 2017